Jebasingh *Renewables (2016)3:8*
DOI 10.1186/s40807-016-0028-2

Renewables: Wind, Water, and Solar
a SpringerOpen Journal

ORIGINAL RESEARCH ARTICLE
Open Access

# Effects of various types of graphite on the thermal conductivity and energy storage properties of ternary eutectic fatty acid-based composite as phase change material

Eanest B. Jebasingh*

**Abstract**

Energy is the greatest challenge facing the environment. Energy efficiency can be improved by energy storage by management of distribution networks, thereby reducing cost and improving energy usage efficiency. This research investigated the energy efficiency achieved by adding various types of graphite (e.g., flake and amorphous) to organic-based ternary eutectic mixtures like capric acid (CA)–myristic acid (MA)–palmitic acid (PA)-based composite phase change materials (PCMs) under the assistance of ultrasonication to improve thermal properties for thermal energy storage. The graphite was surface modified under a Fresnel lens by using concentration of solar rays, then exfoliation of flake graphite by solar irradiation (xG-F) and exfoliation of amorphous graphite by microwave irradiation (xG-A). For each type of graphite exfoliation, ternary eutectic mixtures with mass concentrations of 5 wt% were prepared. The structure, thermal energy storage properties, and thermal stability of the composite PCM were investigated. Thermal conductivity of the samples in the liquid phase was measured using the transient line source method (KD2Pro). The thermal conductivity was increased by loading xG while energy storage properties were slightly decreased. Furthermore, CA–MA–PA + 5 % xG-F has a slightly modified phase change temperature and enthalpy of melting ($T_m = 17.5$ °C; $\Delta H_m = 143.7$ J/g) and freezing ($T_f = 6.7$ °C; $\Delta H_f = 125.5$ J/g); this PCM showed higher thermal conductivity of 0.170 W/(m K), representing an increase of up to 114 % relative to the parent material. On the basis of the above results, xG-A was cheaper than xG-F, but they decrease the energy storage capacity according to DSC results obtained at 2 °C/min. CA–MA–PA/xG-F has more potential for use in low temperature energy storage applications.

**Keywords:** Amorphous graphite, Composite PCM, Energy storage properties, Flake graphite, Thermal conductivity

## Background

Latent heat thermal energy storage (LHTES) has the advantages of high energy storage density and small temperature variation during the phase change process. LHTES has widely employed in various fields including condensation heat recovery, building energy conservation, temperature-regulating textiles, and solar energy system. Phase change materials (PCMs) used in LHTES are generally categorized as inorganic and organic. Inorganic PCMs are salt hydrates, salts, metals, and alloy, have a high heat of fusion, good thermal conductivity, cheap and nonflammable, but their applications are limited due to corrosive to metals, undergo supercooling and phase decomposition. Organic PCMs can be classified into two major categories: paraffin and non-paraffin materials. Paraffin materials have been widely used owing due to desirable thermal characteristics, such as minimal supercooling, varied phase change temperature, low vapor pressure in the melt, good thermal, chemical stability and self-nucleating behavior (Sharma et al. 2009; Baetens et al. 2010; Regin et al. 2008; Kenisarin

*Correspondence: eanestjebasingh@gmail.com
Department of Mechanical Engineeering, TRP Engineering College, Tiruchirappalli 621105, Tamilnadu, India

2010). Among the organic PCMs evaluated fatty acids are promising and then paraffin-based materials fatty acid have suitable phase change temperature, high latent heat capacity and easy manufacturing from common vegetable and animal oils (Oró et al. 2012; Yuan et al. 2014a, b; Karaipekli and Sari 2008; Sari and Kaygusuz 2002; Li et al. 2011; Yanping et al. 2011; Karaipekli and Sarı 2010).

In spite of the desirable properties of organic-based fatty acid PCMs, they have the major drawback of low thermal conductivity that reduces the rate of heat storage and extraction during the melting and solidification cycles. Their thermal conductivity was increased up to 10 % by using an organic fatty acid surfactant such as 5 % sodium myristate, 5 % sodium palmitate, or 5 % sodium stearate (Fauzi et al. 2013). Some inorganic materials have high thermal conductivity e.g., graphite and carbon nanomaterials on addition of treated graphite to the PCM increases their thermal properties and thermal conductivity (Ince et al. 2015; Sari et al. 2008; Sari and Karaipekli 2009; Zhang et al. 2013, 2014a, b, c, 2015; Fang et al. 2010; Liu et al. 2014; Yuan et al. 2014a). Exfoliated graphite (xG) fabricated by exfoliation natural graphite has superior properties mechanical, electrical, and thermal properties (Fukushima et al. 2006). Paraffin/exfoliated graphite (XGnP) is used to enhance the thermal conductivity, latent heat, and heat conductivity of composite PCMs (Kim and Drzal 2009). PCMs with low temperature can be used for cold storage applications like transport temperature-sensitive foods, medical applications, refrigeration and biotechnology industries.

In this paper, exfoliated graphite was produced from flake graphite and amorphous graphite by treating with solar irradiation and microwave irradiation respectively. Then employed as loading content to ternary eutectic fatty acid for improving thermal properties. Then structural morphology, thermal stability, and thermal conductivity of the obtained PCMs were analyzed. Thermal storage properties of the composite PCMs were also investigated.

## Methods

### Materials

Capric acid (CA, 98 % purity), myristic acid (MA, 98 % purity), and palmitic acid (PA, 98 % purity) of analytical grade were bought from Alfa Aesar and Sigma Aldrich. - 320 Mesh flake graphite Purchased from Alfa Aesar and 60 Mesh amorphous graphite from Loba chemie.

### Preparation of exfoliated graphite

Surface treatment of graphite was initially done as shown in Fig. 1. Incoming solar radiation was focused by a Fresnel lens (100 mm diameter) to convert the graphite into a conductive material.

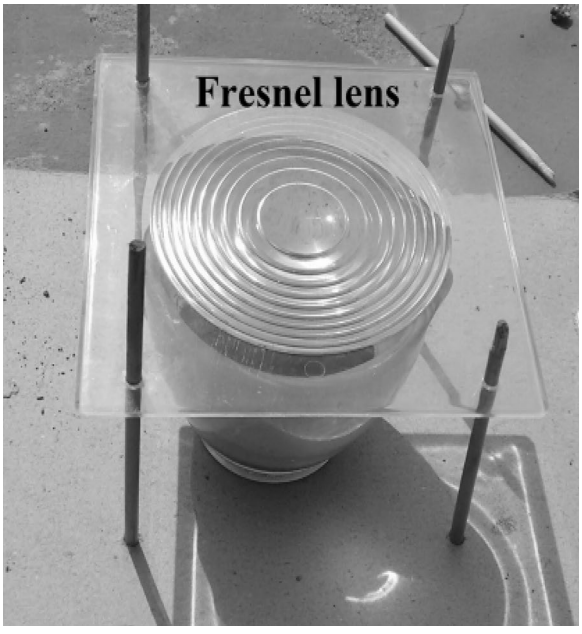


**Fig. 1** Flake graphite in a porcelain dish under a Fresnel lens

#### *Exfoliation of flake (xG-F)*

Thermal exfoliation of flake graphite was performed by brief solar irradiation under a Fresnel lens and brief treatment with nitric acid and potassium permanganate (30 min for solar treatment on natural graphite then 3 min for exfoliation of graphite).

#### *Exfoliation of amorphous (xG-A)*

Exfoliation of amorphous graphite was done by using a homemade microwave oven and brief treatment with nitric acid and potassium permanganate (150 min for solar treatment but they were able to under goes on 1.15 min for exfoliation under microwave oven due to present of oxides).

### Preparation of CA–MA–PA/xG

On the basis of the theoretical mass ratios of CA–MA–PA ternary eutectic mixtures calculated from Eq. (1) (as discussed below), a series of ternary eutectic mixtures were prepared by heating CA–MA–PA (64.8:22.6:12.6) with different CA, MA, and PA contents at a constant temperature of 70 °C, then stirring at 1200 rpm with a magnetic stirrer (2MHL, REMI) to ensure the homogeneity of the mixtures, and slowly cooling to room temperature. The optimum mass ratio of CA–MA–PA to xG-F or xG-A for preparation of CA–MA–PA/xG was 95:5 and obtained under assistance of high speed ultrasonication.

## Characterization

### Analytical methods

The morphology of the xG-F and xG-A was observed by scanning electron microscopy (SEM, VEGA3 TESCAN) at room temperature. SEM images were obtained with an accelerating voltage of 5 kV and working distance of 12 mm. The thermal energy storage properties of CA–MA–PA and CA–MA–PA/xG were analyzed by differential scanning calorimetry (DSC, 200 F3, Maia, NETZSCH); the melting and heat storage behaviors of the pure PCM and composite PCMs were examined at 2 °C/min heating rate in the range of 0–40 °C under a constant flow of nitrogen. Thermogravimetric analysis (STA 409 PL LUXX, NETZSCH) was carried out to determine the decomposition temperature.

### Thermal conductivity analysis

Thermal conductivity of pure CA–MA–PA and CA–MA–PA/xG was determined by using the transient line source method of the KD2Pro thermal conductivity analyzer (Decagon, USA). The sensor used a single needle (KS-1) with a diameter of 1.3 mm and a length of 60 mm.

## Results and discussion

### Mass ratio of CA–MA–PA ternary eutectic mixtures

A eutectic mixture of two or more fatty acids has a lower melting temperature (Oró et al. 2012; Yuan et al. 2014b). Equation (1) was developed by Li et al. (2011) and links the component mass ratios to the melting temperature. Binary eutectic mixtures (Yanping et al. 2011) were calculated first through Eq. (1), and they were near to the partial melting temperature. The theoretical mass ratio of each ternary eutectic mixture was thus calculated on the basis of Eq. (1):

$$T_{\mathrm{m}} = \left[\frac{1}{T_{\mathrm{i}}} - R\ln\frac{X_{\mathrm{i}}}{H_{\mathrm{i}}}\right] \tag{1}$$

where in $T_{\mathrm{m}}$ is the melting temperature of the mixture, $T_{\mathrm{i}}$ is the melting temperature of the initial substance, $X_{\mathrm{i}}$ is the mass of the initial substance, $H_{\mathrm{i}}$ is the latent heat of the initial substance (J mol$^{-1}$), and $R$ is the gas constant (8.315 J mol$^{-1}$ K$^{-1}$). Our main aim was to develop a PCM with a melting temperature below 20 °C (Oró et al. 2012); CA–LA in the mass ratio of 64:36 was obtained at $T_{\mathrm{m}}$ 19.62 °C (Karaipekli and Sarı 2010), but MA–PA in the mass ratio of 60:40 was obtained at $T_{\mathrm{m}}$ 47.08 °C (Fauzi et al. 2013). From Eq. (1), CA–MA–PA with a mass ratio of 64.8:22.6:12.6 (i.e., by replacing the 36 mass ratio lauric acid in CA–LA with MA–PA at a mass ratio of 60:40) was obtained at $T_{\mathrm{m}}$ 15.72 °C. The mass ratio of the actual ternary eutectic mixtures needed to be verified through experiments.

Indeed, the mass ratio of CA–MA–PA ternary eutectic mixture 64.8:22.6:12.6 was obtained at $T_{\mathrm{m}}$ 17.7 °C with little deviation compared with the theoretical value. The discrepancy is due to the errors of the calculation formula and the effect on PCM's purity on the mass ratio and phase change temperature of eutectic mixtures. If there are several endothermic peaks in the DSC curve of a PCM, it means that the PCM is not a eutectic mixture. However, in this case the entire composite has a single endothermic peak which shows that the prepared mixture is homogenous. Therefore, the CA–MA–PA ternary eutectic mixture is a good choice for thermal energy storage for low temperature application.

### Characterization of eutectic PCM composites

The morphology of the ternary eutectic PCM was observed by scanning electron microscopy (SEM, VEGA3 TESCAN) at room temperature. The samples were sputter coated with gold to increase their electrical conductivity. SEM images were obtained at an accelerating voltage of 5 kV and working distance of 12 mm (Fig. 2).

Figure 2a shows a solar-treated exfoliated flake graphite surface with petal-like layered structure. Figure 2b shows a microwave-treated exfoliated amorphous graphite surface with a structure which is different from that of flake graphite. In both cases, the stucture is different to the worm-like structure reported by Wei et al. (2008) for microwave-exfoliated flake graphite surfaces. This result highlights the different effect of the treatment process on the resulting structure.

### Thermal properties of phase change materials

DSC curves of CA–MA–PA and CA–MA–PA/xG were obtained at a heating rate of 2 °C/min (Fig. 3). Table 1 reports the phase change temperatures of CA–MA–PA and CA–MA–PA/xG. Mixing the CA, MA, and PA to prepare a eutectic mixture is a more efficient method to decrease the phase change temperature than using individual components. As a result of the nature of the environment and nature of stirring times the melting and freezing temperatures for CA–MA–PA were measured as 17.7 and 8.4 °C, which differ from the theoretical calculated temperatures. The melting and freezing temperatures of CA–MA–PA/xG-F were 17.5 and 6.7 °C.

The melting temperature and freezing temperatures of CA–MA–PA/xG were slightly lower than those of CA–MA–PA because xG has higher thermal conductivity that accelerates the heat transfer rate of PCM from the outside to inside and decreases the phase change temperature. However, the composite PCM storage ability of CA–MA–PA/xG is decided by the content of

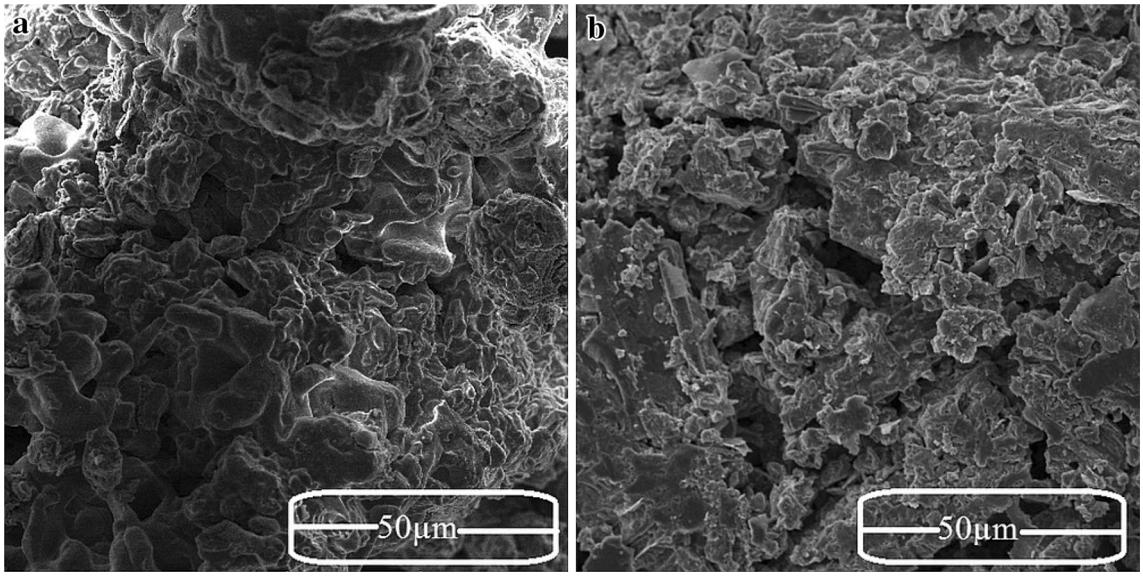


**Fig. 2** SEM images of **a** xG-F and **b** xG-A

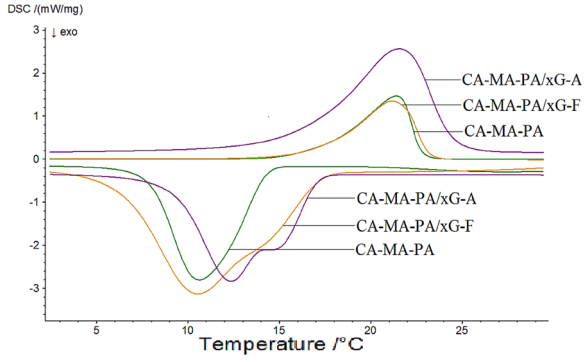


**Fig. 3** DSC curve of CA–MA–PA and composite PCM

CA–MA–PA, which accounts for 95 wt% in CA–MA–PA/xG composite.

Latent heats of melting and freezing were found to be 148.7 and 144.2 J/g for CA–MA–PA but 143.7 and 125.5 J/g for CA–MA–PA/xG-F 5 % composite PCM. In composites containing amorphous graphite, they totally decrease the latent heat. In addition, the latent heats of melting of the composite PCMs are compared with those of other composite PCMs in Table 2.

Figures 4 and 5 show the phase change temperature of the composite PCM and a degree of supercooling, expressed by the difference between melting temperature and freezing temperature obtained from DSC curves. Figure 4 shows that with the increase of xG-F content, the melting points and freezing point of CA–MA–PA/XG-F composites were gradually decreased. Therefore, the degree of supercooling is slightly increased by xG-F 5 % contents. In contrast, Fig. 5 shows that CA–MA–PA/xG-A composites exhibit the opposite tendency, which causes a decrease in the degree of supercooling.

### Thermal conductivity of composite PCM composites

The thermal conductivity of pure CA–MA–PA and CA–MA–PA/xG in the liquid phase was determined by using the transient line source method of the KD2Pro thermal conductivity analyzer at room temperature. The thermal conductivities of the CA–MA–PA/xG composites were remarkably improved relative to CA–MA–PA PCM. As

**Table 1 Thermal properties of PCM**

| PCM | Mass fraction (wt%) | Melting | | Freezing | |
|---|---|---|---|---|---|
| | | $T_{onset}$ (°C) | Latent heat (J/g) | $T_{onset}$ (°C) | Latent heat (J/g) |
| CA–MA–PA | – | 17.7 | 148.7 | 8.4 | 144.2 |
| CA–MA–PA/xG-F | 5 | 17.5 | 143.7 | 6.7 | 125.5 |
| CA–MA–PA/xG-A | 5 | 16.8 | 117.5 | 9.5 | 38.6 |

**Table 2 Comparison of latent heat of melting CA–MA–PA/xG with another component in literature**

| PCM | Material | Melting temp (°C) | Loading % | Pure PCM latent heat (J/g) | PCM composite latent heat (J/g) | Effective ratio (%) | References |
|---|---|---|---|---|---|---|---|
| CA | EG | 27.80 | 20 | 172.42 | 132.64 | 76.9 | Sari et al. (2008) |
| PA | EG | 60.88 | 20 | 194.45 | 148.36 | 76.29 | Sari and Karaipekli (2009) |
| LA–PA–SA | EP | 31.8 | 45 | 151.6 | 81.5 | 53.75 | Zhang et al. (2014c) |
| LA–MA–PA/VMT | EG | 30.6 | 2 | 151.6 | 72.7 | 47.95 | Zhang et al. (2015) |
| LA–MA–PA | EG | 30.94 | 5.3 | 145.3 | 135.9 | 93.53 | Zhang et al. (2013) |
| LA–MA–SA | EG | 29.05 | 7.69 | 140.9 | 137.1 | 97.30 | Liu et al. (2014) |
| Paraffin | xGnP | 50.8 | 5 | 128.8 | 131.5 | 102.57 | Liu et al. (2014) |
| PA–SA | CNT | 53.59 | 8 | 179 | 165 | 92.17 | Zhang et al. (2014b) |
| CA–MA–PA | EG | 18.61 | 7.69 | 135.6 | 128.2 | 94.54 | Yuan et al. (2014b) |
| CA–MA–PA | xG-F | 17.5 | 5 | 148.7 | 143.7 | 96.63 | Current study |

*CNT* carbon nanotube, *EG* expanded graphite, *EP* expanded perlite

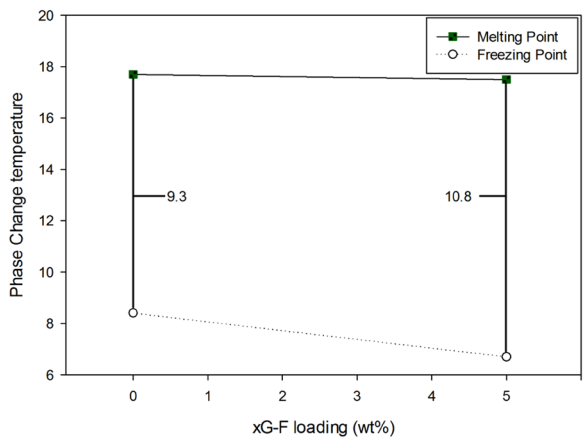


**Fig. 4** Phase change temperature and degree of supercooling of CA–MA–PA/xG-F composites

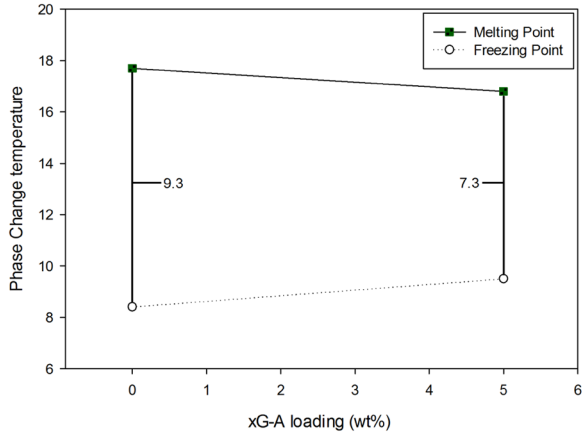


**Fig. 5** Phase change temperature and degree of supercooling of CA–MA–PA/xG-A composites

**Table 3 Thermal conductivity of composite PCM**

| Sample | xG loading content | Reference | 5 % |
|---|---|---|---|
| CA–MA–PA/xG-F | Thermal conductivity W/(m K) | 0.149 | 0.170 |
| | Increase rate (%) | – | 14.09 |
| CA–MA–PA/xG-A | Thermal conductivity W/(m K) | 0.149 | 0.167 |
| | Increase rate (%) | – | 12.08 |

shown in Table 3, the thermal conductivity of CA–MA–PA PCM/xG composites with a mass fraction of 5 % were increased by 14 % by xG-F and 12 % by xG-A. By comparison, Yu et al. (2013) reported that the thermal conductivity of pure paraffin at 65 °C was $k = 0.1504$ W/(m K) and that addition of multi-walled carbon nanotubes caused only a marginal increase in the absolute value of thermal conductivity of 0.012 W/(m K) at the highest loading of 4 wt%.

### Thermal stability of composite PCM

The thermal stability of CA–MA–PA PCM composites was evaluated by means of simultaneous thermal analysis (STA). Thus samples of approximately 2–4 mg were heated in a nitrogen atmosphere from 0 to 500 °C at a heating rate 10 °C/min. CA–MA–PA shows a peak at 283.5 °C and loading of xG-F increased the peak temperature to 288 °C. On the other hand, loading of xG-A in CA–MA–PA composites reduced the peak temperature to 283.0 °C. All the samples behaved similarly and showed that weight loss did not happen below 100 °C; 3.97 % of weight remained after heating at 500 °C (Fig. 6). It can be concluded that the prepared composite PCMs exhibit thermal stability at room temperature.

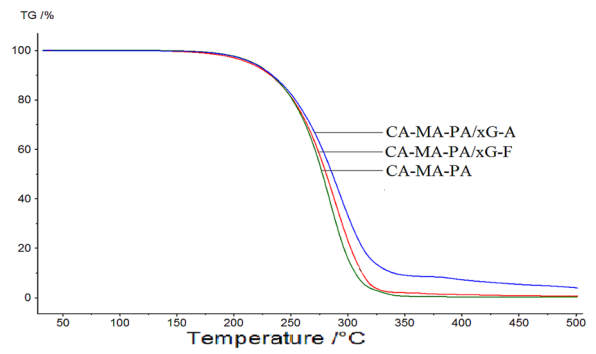


**Fig. 6** TGA curve of CA–MA–PA and composite PCM

## Conclusions

CA–MA–PA composites loaded with xG-F and xG-A were prepared with the aid of sonication to afford PCMs with high thermal conductivity. The melting temperate, freezing temperature, and latent heats of CA–MA–PA/xG-F 95:5 were 17.5 °C, 6.7 °C, 143.7 J/g, and 125.5 J/g respectively. In comparison, the latent heat of CA–MA–PA/xG composites were lower than those of CA–MA–PA. Exfoliated graphite increased the thermal conductivity of CA–MA–PA, and CA–MA–PA/xG-F 5.0 wt% showed an increase in thermal conductivity by 114 %. TGA tests revealed that the prepared composite PCM has a high thermal stability in the working temperature range. Thermal storage and release rates were significantly increased as a result of the increase in thermal conductivity. The results indicate that composite PCMs have great potential for use in low temperature heating and cooling applications.

Received: 22 June 2015 Accepted: 15 February 2016
Published online: 16 March 2016

### References

Baetens, R., Jelle, B. P., & Gustavsen, A. (2010). Phase change materials for building applications: a state-of-the-art review. *Energy Buildings, 42*, 1361–1368.

Fang, G., Li, H., Chen, Z., & Liu, X. (2010). Preparation and characterization of stearic acid/expanded graphite composites as thermal energy storage materials. *Energy, 35*(12), 4622–4626.

Fauzi, H., Metselaar, H. S., Mahlia, T. M. I., Silakhori, M., & Nur, H. (2013). Phase change material: optimizing the thermal properties and thermal conductivity of myristic acid/palmitic acid eutectic mixture with acid-based surfactants. *Appl Therm Eng, 60*(1), 261–265.

Fukushima, H., Drzal, L. T., Rook, B. P., & Rich, M. J. (2006). Thermal conductivity of exfoliated graphite nano composites. *J Therm Anal Calorim, 85*(1), 235–238.

İnce, Ş., Seki, Y., Ezan, M. A., Turgut, A., & Erek, A. (2015). Thermal properties of myristic acid/graphite nanoplates composite phase change materials. *Renew Energy, 75*, 243–248.

Karaipekli, A., & Sari, A. (2008). Capric-myristic acid/vermiculite composite as form-stable phase change material for latent heat thermal energy storage. *Renew Energy, 33*, 2599–2605.

Karaipekli, A., & Sarı, A. (2010). Preparation, thermal properties and thermal reliability of eutectic mixtures of fatty acids/expanded vermiculite as novel form-stable composites for energy storage. *J Ind Eng Chem, 16*, 767–773.

Kenisarin, M. M. (2010). High-temperature phase change materials for thermal energy storage. *Renew Sustain Energy, 14*, 955–970.

Kim, S., & Drzal, L. T. (2009). High latent heat storage and high thermal conductive phase change materials using exfoliated graphite nanoplatelets. *Sol Energy Mater Sol Cells, 93*, 136–142.

Li, M., Wu, Z., & Kao, H. (2011). Study on preparation and thermal properties of binary fatty acid/diatomite shape-stabilized phase change materials. *Sol Energy Mater Sol Cells, 95*(8), 2412–2416.

Liu, C., Yuan, Y., Zhang, N., Cao, X., & Yang, X. (2014). A novel PCM of lauric–myristic–stearic acid/expanded graphite composite for thermal energy storage. *Mater Lett, 120*, 43–46.

Oró, E., De Gracia, A., Castell, A., Farid, M. M., & Cabeza, L. F. (2012). Review on phase change materials (PCMs) for cold thermal energy storage applications. *Appl Energy, 99*, 513–533.

Regin, A. F., Solanki, S. C., & Saini, J. S. (2008). Heat transfer characteristics of thermal energy storage systems using PCM capsules: a review. *Renew Sustain Energy Rev, 12*, 2438–2458.

Sari, A., & Karaipekli, A. (2009). Preparation thermal properties and thermal reliability of palmitic acid/expanded graphite composite as form-stable PCM for thermal energy storage. *Sol Energy Mater Sol Cells, 93*, 571–576.

Sari, A., & Kaygusuz, K. (2001). Thermal performance of myristic acid as a phase change material for energy storage application. *Renew Energy, 24*(2), 303–317.

Sari, A., & Kaygusuz, K. (2002). Thermal performance of palmitic acid as a phase change energy storage material. *Energy Convers Manag, 43*(6), 863–876.

Sari, A., Karaipekli, A., & Kaygusuz, K. (2008). Fatty acid/expanded graphite composites as phase change material for latent heat thermal energy storage. *Energy Sources Part A, 30*, 464–474.

Sharma, A., Tyagi, V. V., Chen, C. R., & Buddhi, D. (2009). Review on thermal energy storage with phase change materials and applications. *Renew Sustain Energy Rev, 13*(2), 318–345.

Wei, T., Fan, Z., Luo, G., Zheng, C., & Xie, D. (2008). A rapid and efficient method to prepare exfoliated graphite by microwave irradiation. *Carbon, 47*, 313–347.

Yanping, Y., Wenquan, T., Xiaoling, C., & Li, B. A. I. (2011). Theoretic prediction of melting temperature and latent heat for a fatty acid eutectic mixture. *J Chem Eng Data, 56*, 2889–2991.

Yu, Z. T., Fang, X., Fan, L. W., Wang, X., Xiao, Y. Q., Zeng, Y., & Cen, K. F. (2013). Increased thermal conductivity of liquid paraffin-based suspensions in the presence of carbon nano-additives of various sizes and shapes. *Carbon, 53*, 277–285.

Yuan, Y., Yuan, Y., Zhang, N., Du, Y., & Cao, X. (2014a). Preparation and thermal characterization of capric–myristic–palmitic acid/expanded graphite composite as phase change material for energy storage. *Mater Lett, 125*, 154–157.

Yuan, Y., Zhang, N., Tao, W., Cao, X., & He, Y. (2014b). Fatty acid as phase change materials:a review. *Renew Sustain Energy Rev, 29*, 482–498.

Zhang, N., Yuan, Y., Wang, X., Cao, X., Yang, X., & Hu, S. (2013). Preparation and characterization of lauric–myristic–palmitic acid ternary eutectic mixtures/expanded graphite composite phase change material for thermal energy storage. *Chem Eng J, 231*, 214–219.

Zhang, N., Yuan, Y., Du, Y., Cao, X., & Yuan, Y. (2014a). Preparation and properties of palmitic-stearic acid eutectic mixture/expanded graphite composite as phase change material for energy storage. *Energy, 78*, 950–956.

Zhang, N., Yuan, Y., Yuan, Y., Cao, X., & Yang, X. (2014b). Effect of carbon nanotubes on the thermal behavior of palmitic–stearic acid eutectic mixtures as phase change materials for energy storage. *Sol Energy, 110*, 64–70.

Zhang, N., Yuan, Y., Yuan, Y., Li, T., & Cao, X. (2014c). Lauric–palmitic–stearic acid/expanded perlite composite as form-stable phase change material: preparation and thermal properties. *Energy Build, 82*, 505–511.

Zhang, N., Yuan, Y., Li, T., Cao, X., Yang, X. (2015). Study on thermal property of lauric–palmitic–stearic acid/vermiculite composite as form-stable phase change material for energy storage. *Adv Mechl Eng, 7*(9), 1–8.